The combined treatment of praziquantel with osteopontin immunoneutralization reduces liver damage in *Schistosoma japonicum*-infected mice

BO-LIN CHEN[1], GUI-YING ZHANG[1]*, SHI-PING WANG[2], QIAN LI[1], MEI-HUA XU[1], YUE-MING SHEN[3], LU YAN[1], HUAN GU[1], JIA LI[1], Y. L. HUANG[4] *and* YI-BING MU[1]

[1] *Department of Gastroenterology, Xiangya Hospital, Central South University, Changsha, 410008, Hunan Province, China*
[2] *Department of Parasitology, College of Xiangya Basic Medicine, Central South University, Changsha, 410008, Hunan Province, China*
[3] *Department of Gastroenterology, Changsha Central Hospital, Changsha, 410004, Hunan Province, China*
[4] *Division of Phamaceutical Science, School of Pharmacy, University of Auckland, Private Bag 92019, Auckland, New Zealand*

(*Received 31 August 2011; revised 12 November 2011; accepted 13 November 2011; first published online 6 February 2012*)

SUMMARY

The aim of this study was to evaluate the therapeutic effects of osteopontin neutralization treatment on schistosome-induced liver injury in BALB/C mice. We randomly divided 100 BALB/C mice into groups A, B, C, D and group E. Mice in all groups except group A were abdominally infected with schistosomal cercariae to induce a schistosomal hepatopathological model. Mice in group C, D and group E were respectively administered with praziquantel, praziquantel plus colchicine and praziquantel plus neutralizing osteopontin antibody. We extracted mouse liver tissues at 3 and 9 weeks after the 'stool-eggs-positive' day, observed liver histopathological changes by haematoxylin-eosin and Masson trichrome staining and detected the expression of osteopontin, alpha-smooth muscle actin (α-SMA) and transforming growth factor-beta (TGF-β1) by immunohistochemistry, RT-PCR and Western blot. We found that praziquantel plus neutralizing osteopontin antibody treatment significantly decreased the granuloma dimension, the percentage of collagen and the expression of osteopontin, α-SMA and TGF-β1 compared to praziquantel plus colchicine treatment in both the acute and chronic stage of schistosomal liver damage ($P<0{\cdot}05$). So we believe that the combined regimen of osteopontin immunoneutralization and anti-helminthic treatment can reduce the granulomatous response and liver fibrosis during the schistosomal hepatopathologic course.

Key words: *Schistosoma japonicum*, granuloma, liver fibrosis, osteopontin, antibody, BALB/C mice.

INTRODUCTION

Schistosomiasis japonica remains a considerable threat to public health and economy in China and some tropical countries despite the remarkable efforts being made for its control (Garjito *et al*. 2008; McManus *et al*. 2009; Bergquist and Tanner, 2010). Schistosomal liver damage begins with the deposition of schistosome eggs in the hepatic sinusoids, leading to the granulomatous inflammation at the early stage and periportal fibrosis at the progressive stage (Burke *et al*. 2009). Human immune response to schistosome eggs is regarded as the major cause of pathology in schistosomiasis, although its original purpose is to eliminate the eggs and neutralize pathogenic antigens. Once the immune response is activated, it is unlikely to be self-limiting because of the self-feedback effect of immunocytes and the cascade reactions they evoke (Coutinho *et al*. 2007; Xu *et al*. 2010). More importantly, hepatic stellate cells are activated by various cytokines, such as transforming growth factor-beta (TGF-β1) during this course, and then they synthesize numerous extracellular matrices, mainly containing collagen, and ultimately lead to liver fibrosis (Gabele *et al*. 2003; Paiva *et al*. 2010; Anthony *et al*. 2010). That is why a standard anti-helminthic treatment is normally ineffective in blocking the continuous schistosomal liver damage and, in addition, praziquantel resistance is a concern (Chapadeiro and Pitanga, 1996; Doenhoff *et al*. 2002). Given that the anti-helminthic therapy alone is not enought for schistosomiasis treatment, to combine with other therapies that limit excessive granulomatous reaction and block the development of liver fibrosis is more important. Because the use of anti-fibrosis drugs in hepatic schistosomiasis is unsatisfactory, finding a new cytokine that is involved in or promotes schistosomal hepatopathology as a new therapeutic target may be a good strategy.

Osteopontin is a secreted phosphorylated glycoprotein involved in physiological and pathological

* Corresponding author: Department of Gastroenterology, Xiangya Hospital, Central South University, Changsha, 410008, Hunan Province, China. Tel: +86 1387 3186462. Fax: +86 0731 84327321. E-mail: guiyingzhang@hotmail.com

Parasitology (2012), **139**, 522–529. Published by Cambridge University Press 2012
doi:10.1017/S0031182011002241

conditions, such as cell migration, granuloma formation, tissue remodelling and immune regulation (O'Regan and Berman, 2000; Giachelli and Steitz, 2000; Chabas, 2005). Our previous study (Chen, 2011) confirmed that the development of schistosomal hepatopathology, including the granuloma formation and liver fibrosis, was accompanied by a dynamic expression of osteopontin, and it correlated well with the expressions of both alpha-smooth muscle actin (α-SMA) and TGF-β1. These results suggest that osteopontin holds a key role in schistosomal hepatopathology.

In the present study, we investigated the potential therapeutic effect of osteopontin immunoneutralization combined with anti-helminthic, and compared this with colchicine, the classic anti-fibrotic drug, on schistosomal liver damage. The granulomatous responses and fibrosis degrees, as well as osteopontin expression and some other potential promoters of liver fibrosis, such as hepatic stellate cells (HSCs) and TGF-β1, were also examined. A comparison of these indices between groups will lead us to evaluate the therapeutic effect of osteopontin immunoneutralization on hepatic schistosomiasis.

MATERIALS AND METHODS

Parasite and laboratory animals

Six-week-old BALB/C female mice were purchased from the Experimental Animal Center (Central South University, Changsha, Hunan, China). All animal experiments were performed in accordance with the Chinese Council on the Animal Care Guide for the Care and Use of Laboratory Animals. *Oncomelania hupensis* harboring *S. japonicum* cercariae were obtained from the Center for Schistosomiasis Control and Prevention (Yueyang, Hunan, China).

Animal treatment

One hundred BALB/C mice were randomly and averagely divided into 5 groups, including a sham control group (group A), model control group (group B), praziquantel treatment group (group C), praziquantel plus colchicine treatment group (group D) and praziquantel plus neutralizing osteopontin antibody treatment group (group E) ($n = 20$ each). Mice in groups B, C, D and group E were percutaneously infected with *S. japonicum* by placing a glass slide carrying 15 ± 1 cercariae in non-chlorine water on its abdomen for 20 min. Mice in group A were treated with non-chlorine water containing no cercariae. All mice were kept at 20–25 °C in a 12-h light/12-h dark cycle with free access to food and water. Mice stools were collected daily after infection, made into smears and observed under optical microscopy in order to identify eggs. The day on which 'stool-eggs-positive' first appeared was defined as 'onset day'. From onset day, praziquantel (500 mg/kg, Nanjing Pharmaceutical Factory Co. Ltd, Nanjing, China) was given daily for 2 days by intragastric administration in groups C, D and group E. And colchicine (200 μg/kg) was given daily by intragastric administration until sacrifice in group D and a neutralizing anti-mouse osteopontin antibody (50 μg/mouse, R&D Systems China Co. Ltd, Shanghai, China) was given once every other day by tail-vein injection for a total of 3 times in group E (Kiefer *et al*. 2010). At 3 weeks (the most suitable time to observe granulomatous responses according to a previous study) and 9 weeks (the time from which liver fibrosis pathology tends to stabilize) after onset day, 10 mice from each group were randomly selected and killed. Liver tissues were extracted and cut into 2 parts: the left lobes of the liver were fixed in a 4% paraformaldehyde solution for 12 h; the remaining portion of the liver was preserved at −80 °C until use.

Histopathological study

Paraformaldehyde-fixed liver specimens were dehydrated in a graded alcohol series. Following xylene treatment, the specimens were embedded in paraffin blocks, cut into 5-μm thick sections, and placed on glass slides. The sections were then stained with haematoxylin-eosin (HE) and Masson trichrome (MT) according to standard procedures. To describe and evaluate liver pathological changes, a pathologist who was blinded to the research design examined 10 different low-power fields of HE- and MT-stained sections (selected fields were in almost the same location) for each mouse. In addition, the percentage of collagen calculated by a multimedia colour image analysis system (Image-Pro Plus 6.0) was measured as a relative objective index to evaluate the degree of liver fibrosis. Each MT-stained section was examined at X100 magnification. Every field analysed contained a granuloma, portal area, or a centrilobular vein. Fibrotic areas were scanned and summed by the software. The percentage of collagen was expressed as the ratio of the collagen-containing area to the whole area, and the result was determined as the mean of 10 different fields of each section. Furthermore, the granuloma dimension was also measured at a magnification of X100 using an ocular micrometer. Only non-confluent granulomas containing eggs in their centres were measured (von Lichtenberg, 1962). Granuloma dimension = maximum width × maximum length. Mean granuloma dimension of each section = sum of all granuloma dimensions in each section/number of granuloma in each section.

Immunohistochemistry

Immunohistochemical staining was performed with the PV-6001/6002 Two-Step IHC Detection Reagent (ZSGB-BIO, China). The sections were

https://doi.org/10.1017/S0031182011002241 Published online by Cambridge University Press

de-waxed, dehydrated, immersed in citrate buffer (0·01 M, pH 6·0), heated at 100 °C in a microwave oven 6 × 2 min, incubated in 3% H_2O_2 in deionized water for 10 min to block endogenous peroxide activity, and washed 2 × 3 min with PBS. The sections were then incubated overnight at 4 °C with antibodies against osteopontin (mouse monoclonal; 1:300; Santa Cruz Biotechnology, USA), α-SMA (mouse monoclonal; 1:300; Santa Cruz Biotechnology, USA), and TGF-β1 (rabbit polyclonal; 1:300; Santa Cruz Biotechnology, USA). After washing 2 × 3 min with PBS, the appropriate second antibody was added to the sections and incubated at 37 °C for 30 min. Then the sections were washed 2 × 3 min with PBS and the colour was developed with DAB for about 5 min. Nuclei were lightly counterstained with haematoxylin. Negative controls included incubation with PBS without the primary antibody. The integral optical density (IOD) was measured with Image-Pro Plus 6.0, and the result was determined as the sum of 5 different fields (1 in the centre and 4 in the periphery) of each section. The IOD of the target protein was defined as the sum of the optical densities of all the positive pixels in the image, which represents the quantity of the targeted protein.

Reverse transcription PCR

Total RNA was extracted from frozen liver tissue with TRIZOL Reagent (Invitrogen, USA). Complementary DNA (cDNA) was synthesized from total RNA using a ReverTra Ace-α-TM First Strand cDNA Synthesis kit (Toyobo, Japan). Relative quantification of target gene expression was performed using the housekeeping gene, glyceraldehyde-3-phosphate dehydrogenase (GAPDH) as an internal control. The primer sequences were as follows: osteopontin forward 5′-ccaggtttctgatgaacagt-3′ and reverse 5′-gtgtgtttccagacttggtt-3′, which yielded a fragment of 193 bp; α-SMA forward 5′-atctggcaccactctttcta-3′ and reverse 5′-gtacgtccagaggcatagag-3′, which yielded a fragment of 191 bp; TGF-β1 forward 5′-agccctggataccaactatt-3′ and reverse 5′-aggaccttgctgtactgtgt-3′, which yielded a fragment of 186 bp; and GAPDH forward 5′-aactttggcattgtggaagg-3′ and reverse 5′-ggatgcagggatgatgttct-3′, which yielded a fragment of 132 bp. For the first step, the following components were mixed to obtain the specified concentrations in a final 20 μl reaction volume: 1 μl of denatured total RNA (1 μg/μl), 4 μl of 5 × RT buffer, 2 μl of dNTP mixture (10 mM), 1 μl of RNase inhibitor (10 U/μl), 10 μl of RNase-free H_2O, 1 μl of Oligo$(dT)_{20}$ (10 pmol/μl), and 1 μl of ReverTra Ace. The reaction was performed at 42 °C for 20 min, followed by 99 °C for 5 min, and 4 °C for 5 min. In the second step, 1 μl of cDNA was mixed with 0·5 μl of each sense and anti-sense primer (100 μmol/l each), 2 μl of dNTP mixture (2 mM), 1·5 μl of $MgCl_2$ (25 mmol/l), 2 μl of 10 × PCR buffer, 0·5 μl of Taq DNA Polymerase (500 U), and 12 μl of PCR H_2O. PCR was performed as follows: denaturation at 95 °C for 5 min; 32 cycles of denaturation at 94 °C for 30 s, annealing at 55 °C for 30 s, elongation at 72 °C for 30 s, and final elongation at 72 °C for 5 min. The PCR products were separated by electrophoresis on 1·5% agarose gels (sample volume: 10 μl, voltage: 120 V) and visualized with ethidium bromide staining and ultraviolet illumination. We used gel optical density analysis software (Gel-Pro 4.0) to scan and calculate the IOD of strips. The relative mRNA expression of osteopontin was represented as the ratio of osteopontin:IOD and GAPDH:IOD, as were the α-SMA and TGF-β1 levels.

Western blotting

Frozen tissue specimens (500 mg) were homogenized on ice in 1 ml of lysate prepared from a Total Protein Extraction kit (ProMab, USA) and then ultrasonicated for 3 × 3 sec. The crude protein fractions were obtained by centrifuging the homogenates at 9000 ***g*** for 10 min at 4 °C. The supernatant was used as the protein fraction. Gel samples were prepared by mixing protein samples with sample buffer and boiling at 100 °C for 3 min. Nuclear and cytoplasmic proteins were separated with 12% sodium dodecyl sulfate-polyacrylamide gel electrophoresis (SDS-PAGE) in running buffer. After electrophoresis, the proteins were transferred to nitrocellulose membrane (Pierce, USA) in transfer buffer at 300 mA constant current for 70 min on ice. Non-specific binding sites were blocked by incubating in PBS containing 5% non-fat milk for 2 h at 37 °C. Membranes were then incubated with primary antibodies (mouse monoclonal osteopontin antibody (1:500) (Santa Cruz Biotechnology, USA), rabbit monoclonal α-SMA antibody (1:200) (Ascend Biotechnology, China), rabbit polyclonal TGF-β1 antibody (1:400) (Santa Cruz Biotechnology, USA) and mouse GAPDH monoclonal antibody (1:1000) (ProMab, USA)) overnight at 4 °C. The membranes were then washed 5 × 4 min with PBS-Tween 20 (PBST) and incubated with secondary antibody (HRP-conjugated goat anti-mouse IgG antibody (1:50000) (Zymed, USA) for osteopontin and GAPDH, HRP-conjugated goat anti-rabbit IgG antibody (1:40000) (Santa Cruz Biotechnology, USA) for TGF-β1 and HRP-conjugated goat anti-rabbit IgG antibody (1:20000) (Santa Cruz Biotechnology, USA) for α-SMA) for 1 h at 37 °C. After the membranes were washed for 5 × 4 min in PBST, enhanced chemiluminescence detection of the target protein was performed. The film was scanned, and the image was analysed with Gel-Pro 4.0. The relative levels of osteopontin were represented as the ratio of osteopontin:IOD and

https://doi.org/10.1017/S0031182011002241 Published online by Cambridge University Press

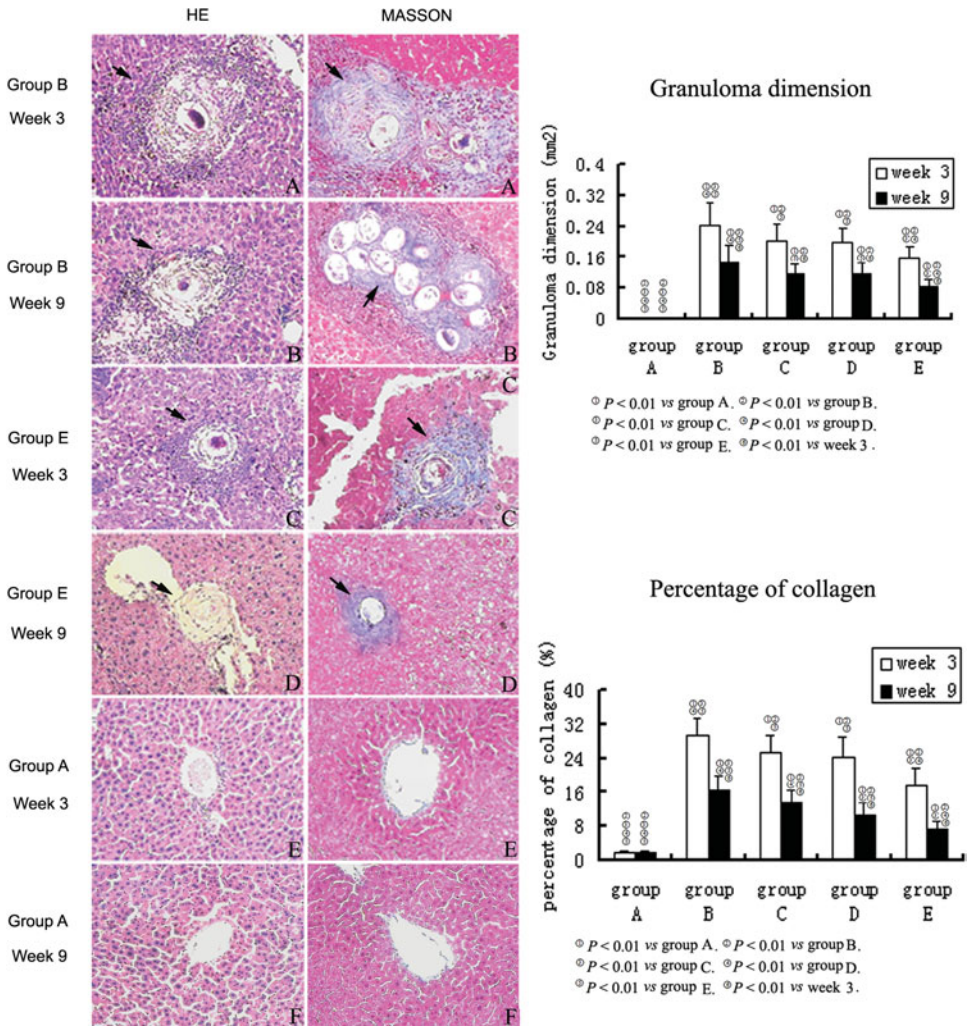

Fig. 1. Representative images of hepatopathological changes in groups A, B and group E over time. Images – HE and MT staining. Graphs – data showing the degree of granuloma formation and liver fibrosis. Arrowheads show granulomas, collagen fibres present a blue colour (MT staining), X100 original magnification. HE, haematoxylin & eosin; MT, Masson trichrome.

GAPDH:IOD, and the same with the α-SMA and TGF-β1 levels.

Statistical analysis

Statistical analysis was performed using SPSS 13.0 software. Data were expressed as means ± S.D. A normality test was performed before statistical analysis. Comparisons between groups and time-points were performed using one-way analysis of variation (ANOVA) (homogeneity of variance: S-N-K; heterogeneity of variance: Tamhane). P values less than 0·01 (heterogeneity of variance) or 0·05 were considered statistically significant.

RESULTS

Schistosomal hepatopathology

Schistosomal hepatopathological changes were described by a senior pathologist according to both HE and MT sections (Fig. 1, images). While group A showed normal hepatocyte morphology (Fig. 1E–F), other groups showed typical characteristics of schistosomal hepatopathology such as granuloma formation and collagen deposition in varying degrees (Fig. 1A–D). At week 3, in group B, numerous inflammatory cells such as neutrophils, lymphocytes and eosinophils infiltrated around schistosome eggs, shaping granulomas; massive collagen fibres wrapped or stretched into granulomas or extended from inflammatory lesions to the lobule (Fig. 1A). While the quantity of inflammatory cells and collagen fibres seemed fewer in group C and group D, group E showed the most obvious reduction in the degree of granuloma responses and fibrosis (Fig. 1C). At week 9, in group B, fibrocytes and collagen fibres became the predominant feature of the granuloma, whereas other cell types diminished in number (Fig. 1B). When there was a decrease in the collagen deposition in group C and group D animals, we could see only sparse collagen interspersed among disintegrated

https://doi.org/10.1017/S0031182011002241 Published online by Cambridge University Press

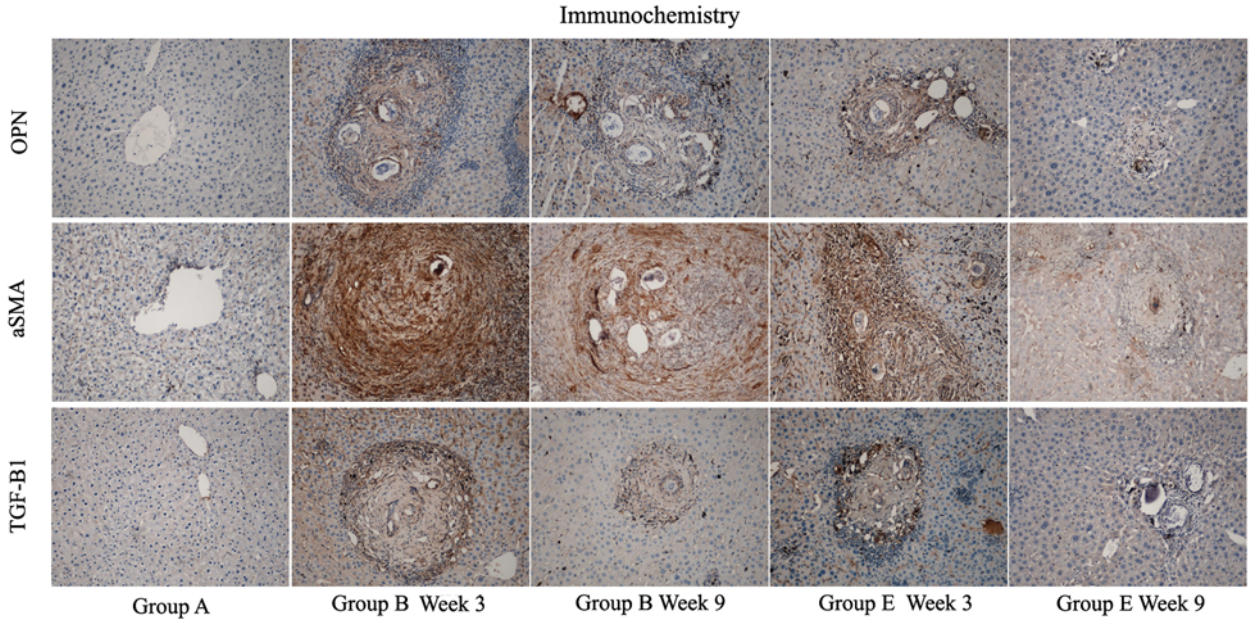

Fig. 2. Representative images and IOD data of immunostaining for osteopontin, α-SMA and TGF-β1 in groups A, B and group E over time. Positive staining presents a yellow brown colour at X100 original magnifications. Table 1 shows detailed IOD data. OPN, osteopontin; SMA: smooth muscle actin; TGF: transforming growth factor; IOD: integral optical density.

granulomas in group E (Fig. 1D). The collagen percentage and the granuloma dimension showed a similar change between groups over time (Fig. 1, graphs).

Expression of osteopontin, α-SMA, and TGF-β1 by immunohistochemistry

Only scarcely distributed cells with traces of the osteopontin-positive staining were seen in group A throughout the experiment (Fig. 2). At week 3, in group B, large numbers of densely osteopontin-stained cells surrounded and infiltrated into the egg granulomas, accumulated in fibrotic areas and stretched along fibrous septum. The quantity of osteopontin gradually reduced following the sequence of groups B, C, D and group E (Fig. 2 and Table 1) ($P<0{\cdot}05$). At week 9, in group B, there were still many osteopontin-stained cells distributed in the fibrotic granulomas and dispersed at the periphery of them. However, the expression had weakened compared to week 3 ($P<0{\cdot}05$) (Fig. 2 and Table 1). The quantity of osteopontin in group E decreased dramatically compared to the other 3 modelling groups (Fig. 2 and Table 1) ($P<0{\cdot}05$). Osteopontin expression showed no significant difference between groups C and group D ($P>0{\cdot}05$) and they both decreased substantially compared to group B ($P<0{\cdot}05$) (Table 1). Although minor discrepancies existed, the expression of α-SMA and TGF-β1 were roughly consistent with osteopontin (Fig. 2). Table 1 shows the IODs of individual immune staining between different groups along the time course. Results are expressed as IOD ($\times 10^2$ or $\times 10^3$) and as the mean $\pm$ S.D.

Expression of osteopontin, α-SMA and TGF-β1 mRNA (RT-PCR) and protein (Western blotting)

Again, similar changes were seen in the expression of mRNA (RT-PCR) and protein (Western blotting) (Fig. 3, left and right, A). The expression of both osteopontin mRNA and protein in group C and group D were significantly decreased compared to group B ($P<0{\cdot}05$). Group E had the lowest osteopontin expression among all the modelling groups ($P<0{\cdot}05$), but its level was still relatively higher than that in group A ($P<0{\cdot}05$). The expression of α-SMA and of TGF-β1 was generally consistent with osteopontin. All detailed data are shown in Fig. 3B–D, left and right.

DISCUSSION

Osteopontin is involved in various pathophysiological events including inflammation and fibrosis (Lorena *et al*. 2006; Morimoto *et al*. 2010). Our previous preliminary study demonstrated that osteopontin played an important role in the progress of schistosomal hepatopathology and strongly correlated with some potential pro-fibrosis factor such as hepatic stellate cells and TGF-β1 (Chen, 2011). Whether it is a positive promoter to schistosomal liver damage, or just a result or manifestation of this pathological process, has not been clarified. Considering the pro-inflammation and pro-fibrosis role osteopontin plays in other diseases (Singh *et al*. 2010; Ueno *et al*. 2010), we hypothesize its role to be the former. Thus, we adopted the method of immunoneutralization to block the action of osteopontin and

https://doi.org/10.1017/S0031182011002241 Published online by Cambridge University Press

Table 1. The IOD of immunostaining in the groups over time

Time	IOD	Group A	Group B	Group C	Group D	Group E
Week 3	OPN($\times 10^2$)	0·665 ± 0·1646 ②③④⑤	27·442 ± 5·54907 ①③④⑥	22·542 ± 3·89467 ①②④⑤	19·024 ± 3·03471 ①②③⑤	14·96 ± 2·79011 ①②③④
	α-SMA($\times 10^2$)	0 ②③④⑤	36·896 ± 6·59257 ①③④⑥	30·187 ± 7·70907 ①②⑤	28·876 ± 7·32312 ①②⑥	22·63 ± 5·73419 ①②③④
	TGF-β1($\times 10^3$)	0·248 ± 0·08917 ②③④⑤	9·285 ± 2·94987 ①③④⑥	7·059 ± 2·28018 ①②⑤	6·826 ± 2·14851 ①②⑥	3·678 ± 1·61896 ①②③④
	OPN($\times 10^2$)	0·7 ± 0·21034② ③④⑤	10·683 ± 2·85227 ①③④⑤⑥	8·034 ± 2·41005 ①②⑤⑥	7·823 ± 2·38668 ①②⑤⑥	4·397 ± 1·90387 ①②③④⑥
Week 9	α-SMA($\times 10^2$)	0 ②③④⑤	23·563 ± 5·43248 ①③④⑤⑥	17·127 ± 4·21454 ①②⑤⑥	17·099 ± 3·98413 ①②⑤⑥	9·392 ± 4·22277 ①②③④⑤
	TGF-β1($\times 10^3$)	0·252 ± 0·10174 ②③④⑤	4·223 ± 1·11353 ①③④⑤⑥	2·781 ± 0·93179 ①②⑥	2·798 ± 0·96148 ①②⑥	2·606 ± 1·0353 ①②⑥

① $P<0·01$ *vs* group A. ② $P<0·01$ *vs* group B. ③ $P<0·01$ *vs* group C. ④ $P<0·01$ *vs* group D. ⑤ $P<0·01$ *vs* group E. ⑥ $P<0·01$ *vs* week 3.

observed the changes in schistosome-induced hepatopathology to confirm our hypothesis and to evaluate the feasibility of osteopontin immunoneutralization as a treatment for hepatic schistosomiasis.

Egg granulomas and liver fibrosis are the most basic characteristics of hepatic schistosomiasis (Gryseels, 2006). Although an elaborate and internationally acknowledged criterion for the evaluation of hepatic schistosomiasis has yet to be established at present, we still find some indices we used in our studies to be applicable and objective. The granuloma dimension undoubtedly reflects the intensity of granulomatous responses that directly determine the degree of fibrosis since fibrosis is originally a tissue-repairing process to previous inflammatory injury (Shimada *et al*. 2010). The percentage of collagen, usually detected with Masson trichrome staining or Sirius red staining, is a common index to assess the extent of collagen deposition (Fornari *et al*. 2011). During the granulomatous responses, hepatic stellate cells transform into activated myofibroblast-like cells characterized by the presence of α-SMA, secreting large amounts of collagen (Reeves and Friedman, 2002; Bartley *et al*. 2006). In addition, TGF-β1, as the most potent fibrogenic cytokine, increases following HSC activation and stimulates the proliferation and activation of HSC to form a self-feedback cascade reaction (Wada *et al*. 2004; Moreira, 2007). We have every reason to believe that an effective therapy for schistosomal liver damage should be able to reduce granulomatous responses and collagen deposition, and even ideally to inhibit HSC activation and TGF-β1 expression.

In this study, we injected neutralizing anti-osteopontin antibody at the time when the schistosome eggs reached the liver, which marks the initiation of hepatic schistosomiasis. We selected 2 time-points for the observation, including 3 weeks and 9 weeks after egg arrival as they, respectively, represent the most obvious acute granulomatous response phase and stable chronic fibrosis phase according to previous studies. Praziquantel was used in all the treatment groups as a basic aetiological treatment. Colchicine, a classical anti-fibrosis drug, was chosen as the control drug. Either colchicine or osteopontin neutralization was combined with praziquantel to compare the treatment effects. As the data showed, praziquantel plus osteopontin neutralization had the most remarkable effect in reducing granulomatous responses and collagen deposition, accompanied with a significant decrease of HSC activation and TGF-β1 expression. This result clearly demonstrates the feasibility and rationality of osteopontin immunoneutralization for the treatment of schistosomal liver damage. In addition, it further confirms that osteopontin has a pro-inflammation and pro-fibrosis effect in hepatic schistosomiasis, although the detailed mechanisms were still not entirely clear. Some other reports seem to provide a few clues: a

https://doi.org/10.1017/S0031182011002241 Published online by Cambridge University Press

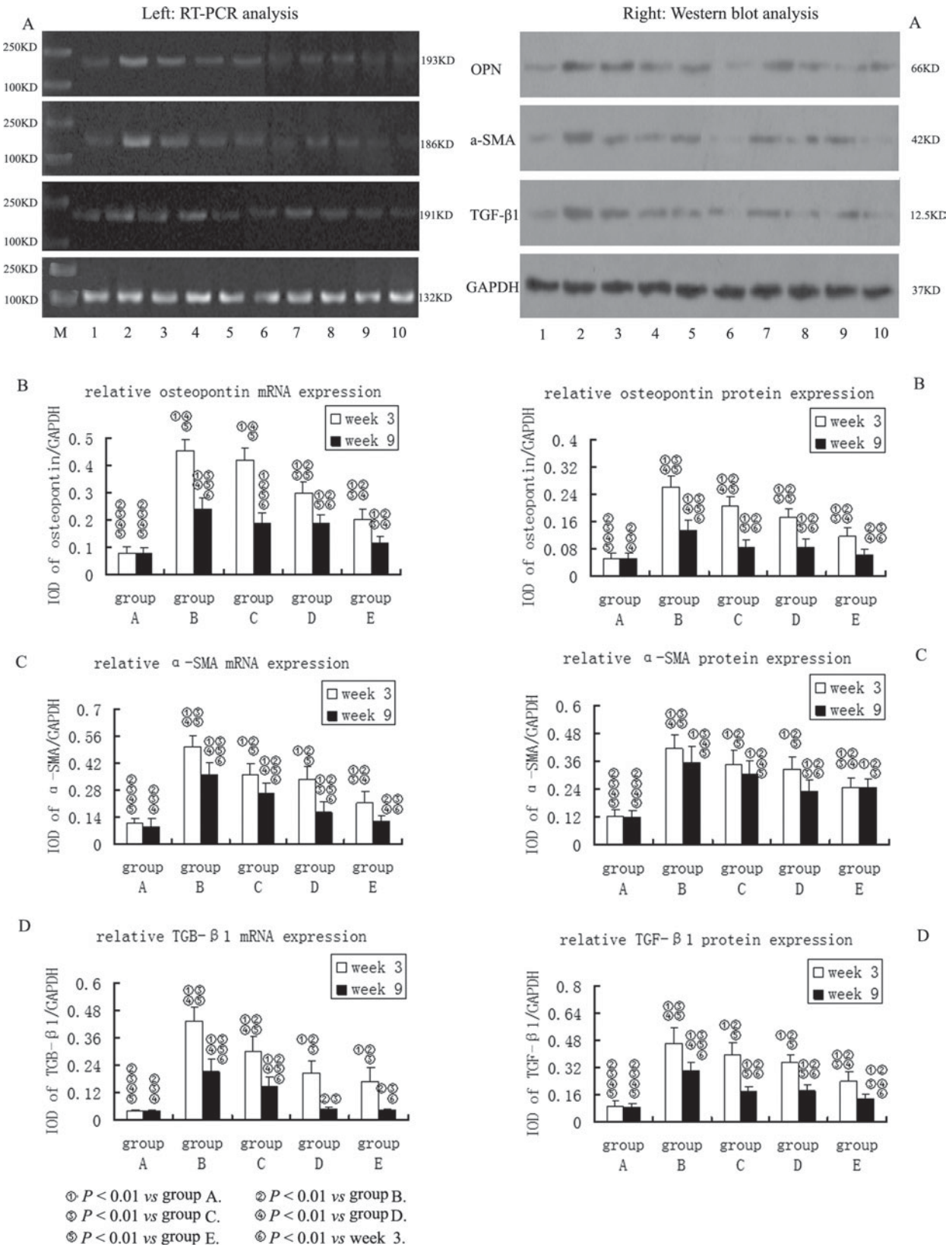

Fig. 3. Profiles of osteopontin, α-SMA and TGF-β1 mRNA (RT-PCR) and protein (Western blotting) expression. Left. Expression of the targeted mRNAs. Letter M representing DNA marker. Numbers 1–5 representing groups A, B, C, D and group E at week 3. Numbers 6–10 representing groups A, B, C, D and group E at week 9. Right. Expression of the proteins. Numbers 1–5 representing groups A, B, C, D and group E at week 3. Numbers 6–10 representing groups A, B, C, D and group E at week 9.

https://doi.org/10.1017/S0031182011002241 Published online by Cambridge University Press

review summarizing the pathophysiological role of osteopontin in hepatic inflammation and toxicity concludes that osteopontin acts as a mediator of various inflammatory cell infiltrations, including lymphocytes, neutrophils, and macrophages (Ramaiah and Rittling, 2008). A recent *in vitro* study demonstrated that osteopontin is required for the differentiation and activity of myofibroblasts that are formed in response to the profibrotic cytokine TGF-β1 (Lenga *et al*. 2008).

In summary, through this study, osteopontin's role as a positive promoter of schistosomal liver damage is further confirmed. Immunoneutralization aimed at osteopontin, in combination with praziquantel for the aetiological treatment, significantly alleviates schistosomal damage in the liver. This combined regimen of osteopontin immunoneutralization and aetiological anti-helminthic treatment reveals a new strategy and has the potential for a more effective treatment of hepatic schistosomiasis, even though it will be a long way for this regimen to become a new clinical therapy for patients with schistosomiasis.

FINANCIAL SUPPORT

This study was supported by grants from the National Natural Science Foundation of China (81072038/H1617) and the Post-Graduate Degree Thesis Innovation Foundation of Central South University, Changsha, P.R. China.

REFERENCES

Anthony, B., Allen, J. T., Li, Y. S. and McManus, D. P. (2010). Hepatic stellate cells and parasite-induced liver fibrosis. *Parasites & Vectors* **3**, 60. doi: 10.1186/1756-3305-3-60.

Bartley, P. B., Ramm, G. A., Jones, M. K., Ruddell, R. G., Li, Y. and McManus, D. P. (2006). A contributory role for activated hepatic stellate cells in the dynamics of Schistosoma japonicum egg-induced fibrosis. *International Journal for Parasitology* **36**, 993–1001. doi: 10.1016/j.ijpara.2006.04.015.

Bergquist, R. and Tanner, M. (2010). Controlling schistosomiasis in Southeast Asia: a tale of two countries. *Advances in Parasitology* **72**, 109–144. doi: 10.1016/S0065-308X(10)72005-4.

Burke, M. L., Jones, M. K., Gobert, G. N., Li, Y. S., Ellis, M. K. and McManus, D. P. (2009). Immunopathogenesis of human schistosomiasis. *Parasite Immunology* **31**, 163–176. doi: 10.1111/j.1365-3024.2009.01098.x.

Chabas, D. (2005). Osteopontin, a multi-faceted molecule. *Medecine Sciences (Paris)* **21**, 832–888. doi: 10.1051/medsci/20052110832.

Chapadeiro, E. and Pitanga, L. C. (1996). On the reversal of schistosomiasis hepatic fibrosis after specific therapy. Histopathologic study. *Revista da Sociedade Brasileira de Medicina Tropical* **30**, 53–56.

Chen, B. L., Zhang, G. Y., Yuan, W. J., Wang, S. P., Shen, Y. M., Yan, L., Gu, H. and Li, J. (2011). Osteopontin expression is associated with hepatopathologic changes in *Schistosoma japonicum*–infected mice. *World Journal of Gastroenterology* **17**, 5075–5082.

Coutinho, H. M., Acosta, L. P., Wu, H. W., McGarvey, S. T., Su, L., Langdon, G. C., Jiz, M. A., Jarilla, B., Olveda, R. M., Friedman, J. F. and Kurtis, J. D. (2007). Th2 cytokines are associated with persistent hepatic fibrosis in human *Schistosoma japonicum* infection. *The Journal of Infectious Diseases* **195**, 288–295. doi: 10.1086/510313.

Doenhoff, M. J., Kusel, J. R., Coles, G. C. and Cioli, D. (2002). Resistance of *Schistosoma mansoni* to praziquantel: is there a problem? *Transactions of the Royal Society of Tropical Medicine and Hygiene* **96**, 465–469.

Fornari, A., Rhoden, E. L., Zettler, C. G., Ribeiro, E. P. and Rhoden, C. R. (2011). Effects of the chronic use of finasteride and doxazosin mesylate on the histomorphometric characteristics of the prostate: experimental study in rats. *International Urology and Nephrology* **43**, 39–45. doi: 10.1007/s11255-010-9770-3.

Gabele, E., Brenner, D. A. and Rippe, R. A. (2003). Liver fibrosis: signals leading to the amplification of the fibrogenic hepatic stellate cell. *Frontiers in Bioscience* **8**, 69–77. doi: 10.2741/887.

Garjito, T. A., Sudomo, M., Abdullah, Dahlan, M. and Nurwidayati, A. (2008). Schistosomiasis in Indonesia: past and present. *Parasitology International* **57**, 277–280. doi: 10.1016/j.parint.2008.04.008.

Giachelli, C. M. and Steitz, S. (2000). Osteopontin: A versatile regulator of inflammation and biomineralization. *Matrix Biology* **19**, 615–622. doi: 10.1016/S0945-053X(00)00108-6.

Gryseels, B., Polman, K., Clerinx, J. and Kestens, L. (2006). Human schistosomiasis. *The Lancet* **368**, 1106–1118. doi: 10.1016/S0140-6736(06)69440-3.

Kiefer, F. W., Zeyda, M., Gollinger, K., Pfau, B., Neuhofer, A., Weichhart, T., Säemann, M. D., Geyeregger, R., Schlederer, M., Kenner, L. and Stulnig, T. M. (2010). Neutralization of osteopontin inhibits obesity-induced inflammation and insulin resistance. *Diabetes* **59**, 935–946. doi: 10.2337/db09-0404.

Lenga, Y., Koh, A., Perera, A. S., McCulloch, C. A., Sodek, J. and Zohar, R. (2008). Osteopontin expression is required for myofibroblast differentiation. *Circulation Research* **102**, 319–327. doi: 10.1161/circresaha.107.160408.

Lorena, D., Darby, I. A., Gadeau, A. P., Leen, L. L., Rittling, S., Porto, L. C., Rosenbaum, J. and Desmoulière, A. (2006). Osteopontin expression in normal and fibrotic liver. Altered liver healing in osteopontin-deficient mice. *Journal of Hepatology* **44**, 383–390. doi:10.1016/j.jhep.2005.07.024.

McManus, D. P., Li, Y., Gray, D. J. and Ross, A. G. (2009). Conquering 'snail fever': schistosomiasis and its control in China. *Expert Review of Anti-infective Therapy* **7**, 473–485. doi: 10.1586/eri.09.17.

Moreira, R. K. (2007). Hepatic stellate cells and liver fibrosis. *Archives of Pathology & Laboratory Medicine* **131**, 1728–1734.

Morimoto, J., Kon, S., Matsui, Y. and Uede, T. (2010). Osteopontin; as a target molecule for the treatment of inflammatory diseases. *Current Drug Targets* **11**, 494–505.

O'Regan, A. and Berman, J. S. (2000). Osteopontin: A key cytokine in cell mediated and granulomatous inflammation. *International Journal of Experimental Pathology* **81**, 373–390. doi: 10.1046/j.1365-2613.2000.00163.x.

Paiva, L. A., Maya-Monteiro, C. M., Bandeira-Melo, C., Silva, P. M., El-Cheikh, M. C., Teodoro, A. J., Borojevic, R., Perez, S. A. and Bozza, P. T. (2010). Interplay of cysteinyl leukotrienes and TGF-β in the activation of hepatic stellate cells from *Schistosoma mansoni* granulomas. *Biochimica et Biophysica Acta* **1801**, 1341–1348. doi: 10.1016/j.bbalip.2010.08.014.

Ramaiah, S. K. and Rittling, S. (2008). Pathophysiological role of osteopontin in hepatic inflammation, toxicity, and cancer. *Toxicological Sciences* **103**, 4–13. doi: 10.1093/toxsci/kfm246.

Reeves, H. L. and Friedman, S. L. (2002). Activation of hepatic stellate cells – a key issue in liver fibrosis. *Frontiers in Bioscience* **7**, d808–d826. doi: 10.2741/reeves.

Shimada, M., Kirinoki, M., Shimizu, K., Kato-Hayashi, N., Chigusa, Y., Kitikoon, V., Pongsasakulchoti, P. and Matsuda, H. (2010). Characteristics of granuloma formation and liver fibrosis in murine schistosomiasis mekongi: a morphological comparison between *Schistosoma mekongi* and *S. japonicum* infection. *Parasitology* **137**, 1781–1789. doi: 10.1017/S0031182010000806.

Singh, M., Foster, C. R., Dalal, S. and Singh, K. (2010). Osteopontin: role in extracellular matrix deposition and myocardial remodeling post-MI. *Journal of Molecular and Cellular Cardiology* **48**, 538–543. doi: 10.1016/j.yjmcc.2009.06.015.

Ueno, T., Miyazaki, E., Ando, M., Nureki, S. and Kumamoto, T. (2010). Osteopontin levels are elevated in patients with eosinophilic pneumonia. *Respirology* **15**, 1111–1121. doi: 10.1111/j.1440-1843.2010.01825.x.

von Lichtenberg, F. V. (1962). Host response to eggs of *S. mansoni*. I. Granuloma formation in the unsensitized laboratory mouse. *The American Journal of Pathology* **41**, 711–731.

Wada, W., Kuwano, H., Hasegawa, Y. and Kojima, I. (2004). The dependence of transforming growth factor-beta-induced collagen production on autocrine factor activin A in hepatic stellate cells. *Endocrinology* **145**, 2753–2759. doi: 10.1210/en.2003-1663.

Xu, X., Wen, X., Chi, Y., He, L., Zhou, S., Wang, X., Zhao, J., Liu, F. and Su, C. (2010). Activation-induced T helper cell death contributes to Th1/Th2 polarization following murine *Schistosoma japonicum* infection. *Journal of Biomedicine and Biotechnology* **2010**, 202397. doi: 10.1155/2010/202397.